

Identifying entanglement using quantum “ghost” interference and imaging

Milena D’Angelo,^{1,*} Yoon-Ho Kim,^{2,†} Sergei P. Kulik,^{1,‡} and Yanhua Shih¹

¹*Department of Physics, University of Maryland, Baltimore County, Baltimore, Maryland, 21250*

²*Center for Engineering Science Advanced Research, Computer Science & Mathematics Division, Oak Ridge National Laboratory, Oak Ridge, TN 37831*

(Dated: August 20, 2003)

We report a quantum interference and imaging experiment which shows quantitatively that Einstein-Podolsky-Rosen (EPR) type entangled two-photon states exhibit both momentum-momentum and position-position correlations, stronger than any classical correlation. We show indeed that the product of the uncertainties in the sum of momenta and in the difference of positions of the entangled two-photon satisfies an EPR-type non-classicality condition. Such a measurement provides a direct way to distinguish between quantum entanglement and classical correlation in continuous variables.

PACS numbers: 42.50.Xa, 03.65.Ud, 42.50.St, 42.65.Lm

The concept of multi-particle quantum entanglement, one of the most surprising consequences of quantum mechanics, was introduced in the very early days of quantum theory [1, 2]. Since the development of spontaneous parametric down-conversion (SPDC) as an efficient source of two-photon entangled states in late 1980’s [3], many experiments have been realized to exhibit and, afterwards, to exploit the very surprising quantum effects of entangled states for secure communication, information processing, and metrology [4].

Some of the most intriguing effects of two-photon entanglement in SPDC are quantum ‘ghost’ interference and imaging [5, 6]. These effects are of great importance in potential applications like quantum metrology and lithography [7, 8, 9]. Recently, it has been claimed that the two-photon ‘ghost’ image can be achieved using a pair of classically \mathbf{k} -vector correlated optical pulses [10]. Ref. [10], therefore, raises interesting questions about fundamental issues of quantum theory, namely: (i) to what extent can quantum entanglement be simulated with classically correlated systems? and (ii) how can we experimentally make a distinction between them?

In this Letter, we report an experiment which sheds light on these two tightly related questions. Our idea is to exploit quantum interference-imaging effects to verify experimentally an EPR-type inequality, which allows distinguishing quantum entanglement from classical correlation in continuous variables. By analyzing the results of a two-photon interference and imaging experiment, we show quantitatively that *entangled* two-photon pairs exhibit both momentum-momentum and position-position EPR-type correlations, which are stronger than any classical correlation. Pairs of particles having a per-

fect *classical correlation* in momentum (or position) automatically do not exhibit any correlation in position (or momentum), due to the uncertainty principle. Our experiment, therefore, shows that two-photon entanglement in momentum and position variables can be verified experimentally and suggests that the degree of entanglement can be quantified through the EPR-type non-classicality/non-locality condition.

Consider a pair of EPR-correlated particles. The whole system is then described in such a way that the sum of the momenta (or difference in the positions) is completely known but the momentum (or position) of each particle is completely undefined [2]. As pointed out by EPR, the most peculiar characteristic of EPR-entanglement is its independency on the selected basis: entanglement in momentum automatically implies entanglement in position. In EPR notation, the quantum state of entangled two-particle pairs can indeed be written as

$$\Psi(x_1, x_2) = \int u_p(x_1)\psi_p(x_2)dp = \int v_x(x_1)\phi_x(x_2)dx,$$

where x_1 (x_2) is the variable used to describe particle 1 (particle 2), $u_p(x_1)$ ($\psi_p(x_2)$) is the momentum eigenfunction for particle 1 (particle 2), and $v_x(x_1)$ ($\phi_x(x_2)$) is the corresponding position eigenfunction obtained by Fourier transform of $u_p(x_1)$ ($\psi_p(x_2)$).

As suggested by EPR, an important consequence of entanglement appears explicitly by considering the case in which $u_p(x_1)$ ($\psi_p(x_2)$) is a plane wave. In this case the EPR entangled state assumes an interesting form:

$$\Psi(x_1, x_2) = \int \delta(p_1 + p_2)e^{ip_1x_1/\hbar}e^{ip_2x_2/\hbar}dp_1dp_2 = \hbar\delta(x_1 - x_2). \quad (1)$$

A perfectly EPR-correlated particle pair should therefore be characterized by both the values $\Delta(\mathbf{k}_1 + \mathbf{k}_2) = 0$ and $\Delta(\mathbf{r}_1 - \mathbf{r}_2) = 0$. However, even when these uncertainties are different from zero (non-perfect entanglement), they still satisfy the inequality,

$$\Delta(\mathbf{k}_1 + \mathbf{k}_2)\Delta(\mathbf{r}_1 - \mathbf{r}_2) < 1. \quad (2)$$

*Electronic address: dmilena1@umbc.edu

†Electronic address: yokim@umbc.edu

‡Permanent address: Department of Physics, Moscow State University, Moscow, Russia.

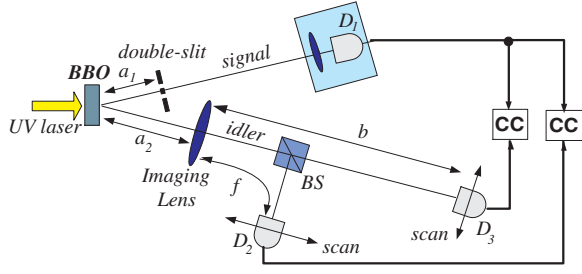


FIG. 1: Schematic of the experimental setup for observing the two-photon ‘ghost’ interference and ‘ghost’ image. For simplicity, the prism to remove the pump and the polarizing Thompson prism are not shown. The double-slit has width $a = 0.165$ mm and slit distance $d = 0.4$ mm. The imaging lens has focal length $f = 510$ mm. The collection lens in the detector package on the signal side has $f = 500$ mm. Relevant distances in this experiment are $a_1 = 32.5$ cm, $a_2 = 46.5$ cm, and $b = 142$ cm. CC is the coincidence circuit.

This result comes directly from the *coherent superposition* of two-particle amplitudes, which cannot be achieved by any classically correlated pairs of particles, as discussed in more details later.

A non-classicality relation for a two-mode squeezed state, which is somewhat analogous to Eq. (2), has been verified experimentally [11]. To the best of our knowledge, however, a direct experimental verification of Eq. (2) via the measurement of $\Delta(\mathbf{k}_1 + \mathbf{k}_2)$ from a quantum interference experiment and the measurement of $\Delta(\mathbf{r}_1 - \mathbf{r}_2)$ from a quantum imaging experiment, has not been reported in literature. In this paper, we report an experimental verification of Eq. (2) utilizing quantum ‘ghost’ interference and image effects of entangled two-photon pairs. Both quantum interference and imaging are realized using the same SPDC source.

Let us first examine whether SPDC two-photon pairs would really exhibit EPR-type entanglement. Under the assumption that the pump beam is a plane wave and the transverse dimensions of the pump beam and the down-conversion crystal are much bigger than the wavelengths of the photons, the quantum state of the SPDC two-photon pairs can be written as [12, 13]:

$$|\Psi\rangle = \sum_{s,i} \delta(\omega_s + \omega_i - \omega_p) \delta(\mathbf{k}_s + \mathbf{k}_i - \mathbf{k}_p) a_s^\dagger a_i^\dagger |0\rangle, \quad (3)$$

where ω_j and \mathbf{k}_j (with $j = s, i, p$) are the frequency and wavevector of the signal (s), idler (i), and pump (p), respectively, and a_s^\dagger (a_i^\dagger) is the creation operator for the signal (idler) photon. Since in this Letter we are only interested in the transverse correlation of the entangled two-photon pairs [13], the quantum state used in our experiment is indeed very close to the one of the original EPR-type entangled pairs of particles. Verification of non-classicality using Eq. (2) should then be possible through the measurement of quantum interference and image realized with this source.

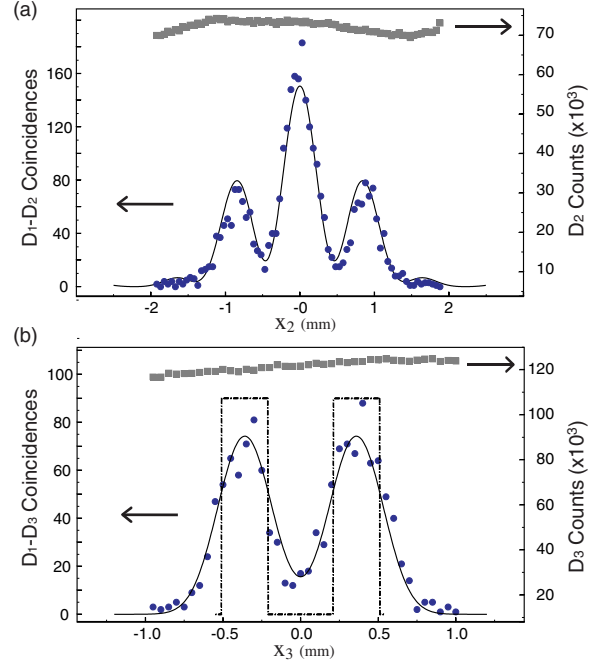


FIG. 2: Experimental data. (a) ‘Ghost’ interference-diffraction pattern. (b) ‘Ghost’ image pattern. Dashed line represents the theoretically perfect image of the slit. Solid lines are fits to the data based on theoretical predictions, taking into account the size of the detectors and the gaussian profile of the pump beam. $\Delta(\mathbf{k}_1 + \mathbf{k}_2)$ and $\Delta(\mathbf{r}_1 - \mathbf{r}_2)$ are evaluated from each of the fitting curves.

A schematic of the experimental setup can be seen in Fig. 1. The 351.1 nm line of an argon ion laser is used to pump a BBO crystal cut for type-II collinear degenerate parametric down conversion. Pairs of orthogonally polarized signal and idler photons at central wavelength $\lambda_i = \lambda_s = 702.2$ nm, which are entangled in momentum, emerge from the crystal almost collinearly with the pump laser. After the crystal, the pump laser beam is separated from the SPDC beam by a quartz dispersion prism. A polarization beam splitting Thompson prism separates the co-propagating signal and idler into two separate spatial modes. The signal photon propagates through a double-slit toward a detector package consisting of a collection lens and a single photon detector placed in its focus (D_1). The idler photon propagates freely before being collected by the imaging lens. A 50-50 beam splitter (BS) is inserted after the lens. The reflected and transmitted photons are then detected by single photon detectors D_2 and D_3 , respectively. Each of them is mounted on an encoder driver to scan its own transverse plane. A spectral filter centered at 702.2 nm with 3 nm bandwidth precedes each detector. The output pulses of the detectors are sent to a coincidence circuit (CC). Coincidences are measured between D_1 and D_2 and between D_1 and D_3 .

This setup therefore allows to measure both ‘ghost’ interference-diffraction and ‘ghost’ image patterns of the

double-slit [5, 6]. The results are shown in Fig. 2. The single counts on both D_2 and D_3 , which are scanned in the transverse direction, show no features at all. This makes sense because no object is inserted in the propagation path of the idler photon. The single counting rate of D_1 , when scanned in the transverse direction, did not show any interference fringes as well: only a wide bell-shaped pattern was observed. This result is due to the fact that biphotons are generated with all possible momenta \mathbf{k}_i and \mathbf{k}_s such that $\mathbf{k}_s + \mathbf{k}_i = \mathbf{k}_p$ is satisfied. In our experiment, the divergence of the SPDC beam $\Delta(\theta)$, which takes into account the filters bandwidth, the dispersion in the crystal, and the phase matching condition, is such that: $\Delta(\theta) \approx 2.6 \text{ mrad} \gg \lambda/d$, where $d = 0.4 \text{ mm}$ is the distance between the slits and $\lambda = 702.2 \text{ nm}$ is the central wavelength of the SPDC photons. Under this condition, the first order interference-diffraction pattern on D_1 is simply washed out.

It is, however, possible to observe a ‘ghost’ interference-diffraction pattern when counting coincidences between D_1 and D_2 (D_1 is fixed and D_2 is scanned in the focal plane of the imaging lens) and to observe a ‘ghost’ image pattern in coincidences between D_1 and D_3 (D_1 is, again, fixed and D_3 is scanned in the image plane) [5, 6]. In both cases, it is important to keep in mind the role of the fixed detector D_1 . For ‘ghost’ interference-diffraction measurement, D_1 detects all the signal photons whose diffraction pattern has a contribution different from zero in the focus of the collection lens. Counting coincidences while scanning D_2 in the focal plane of the imaging lens, allows to select between all the randomly distributed idler photons, the ones corresponding to the detected \mathbf{k}_s ($\mathbf{k}_i = \mathbf{k}_p - \mathbf{k}_s$). As shown in Ref. [5] we then expect the coincidence counting rate to be

$$R_c(x_2) \propto \text{sinc}^2[x_2\pi a/(\lambda f_2)]\cos^2[x_2\pi d/(\lambda f_2)], \quad (4)$$

where x_2 is the transverse position of detector D_2 in the focal plane of L_2 .

Figure 2(a) shows the ‘ghost’ interference measurement. The continuous line in Figure 2(a) is a fitting of the experimental data, which takes into account both the finite size of the detectors, the divergence of the pump and the less-than-perfect correlation between signal and idler. The fitting has been realized using the visibility V of the interference pattern ($\propto 1 + V\cos[2x_2\pi d/(\lambda f_2)]$) as the fitting parameter. We find for the less-than-perfect transverse correlation between signal and idler photons:

$$\Delta(k_{x_s} + k_{x_i}) = 2.5 \pm 0.6 \text{ mm}^{-1}.$$

In an analogous way, we may also obtain $\Delta(\mathbf{r}_s - \mathbf{r}_i)$ by studying the ‘ghost’ image obtained by measuring coincidences between D_1 and D_3 , see Fig. 2(b). It is well known that, to observe a ‘ghost’ image, the two-photon Gaussian thin lens equation, $1/s_i + 1/s_o = 1/f$, where $s_i = b$ and $s_o = a_1 + a_2$ is the distance from the object back to

the crystal and forward to the imaging lens L_2 , should be satisfied [6]. To understand ‘ghost’ image properly, it is important to keep in mind the coherent superposition of biphoton amplitudes resulting from the SPDC state. Indeed, it is the *coherent superposition* (entanglement) that allows exploiting the momentum-momentum correlation to obtain an image (position-position correlation) by simply changing the observation plane (D_3 , instead of D_2). The two-photon Gaussian thin lens equation is the explicit manifestation of the position-position correlation and it appears as a general law in our setup due to the entangled nature of our source [13, 14].

Since the detected signal photons are the ones that have not been stopped by the double slit, the role of the double slit is to measure the localization of the signal with an uncertainty $\Delta(x_s)$, equal to the slit width a . On the other side, detector D_3 detects the idler photons corresponding to the detected signal photons. In the ideal case, counting coincidences, we would obtain two rectangles of width $a' = ma$, and center-to-center distance $d' = md$, where $m = s_i/s_o$ is the magnification. In our case $m = 1.8$, $a = 0.165 \text{ mm}$, $d = 0.4 \text{ mm}$ and the corresponding ideal result ($a' = 0.297 \text{ mm}$, $d' = 0.72 \text{ mm}$) is plotted as dashed line in Fig. 2(b). To take into account a more realistic situation we fit the data with the convolution of the double slit with a Gaussian function that takes into account the finite size of the detectors. The comparison of the resulting fitting curve with the theoretical result, dashed line in Fig. 2(b), allows to evaluate $\Delta(x_s - x_i)$, as the difference between the FWHM of the two curves:

$$\Delta(x_s - x_i) = 0.11 \pm 0.02 \text{ mm}.$$

Note that the center-to-center distance between the bell-shaped fitting curve and the two rectangles is exactly the same (0.72 mm). The imperfect correlation in position is evidently smaller than the distance between the two slits.

Finally, the product of the uncertainties evaluated from the two sets of measurements described above, gives:

$$\Delta(k_{x_s} + k_{x_i})\Delta(x_s - x_i) = 0.3 \pm 0.1 < 1. \quad (5)$$

The non-classicality condition introduced in Eq. (2) is then satisfied for the momentum and position variables of entangled photons of SPDC.

As we mentioned earlier, this result is a direct consequence, if not the definition, of quantum correlation: particles that are entangled in momentum are automatically entangled in position. Only entangled particles can satisfy such inequality. An interesting way of understanding this result is the following. The Fourier transform of an entangled state such as the one given in Eq. (1) and (3), can be factorized by introducing the variables $\mathbf{k}_1 + \mathbf{k}_2$ and $\mathbf{k}_1 - \mathbf{k}_2$. The corresponding Fourier transformed variables

are $\mathbf{r}_1 + \mathbf{r}_2$ and $\mathbf{r}_1 - \mathbf{r}_2$, respectively. Since $\mathbf{k}_1 + \mathbf{k}_2$ and $\mathbf{r}_1 - \mathbf{r}_2$ are not Fourier conjugate variables, the product of their uncertainties can definitely be smaller than one (as shown in Eq. 2).

Let us now consider the case of two particles or beams classically correlated in momentum. An example of such a source is given by a pair of bounded identical guns which emit (quantum) particles while rotating simultaneously, in such a way that the momenta of the two particles are always equal in modulus but with opposite direction. Each pair of *independent but correlated* particles, fired at a certain angle at a given time, may be described by:

$$|\Psi_j\rangle_{12} = a_1^\dagger(\mathbf{k}_j) a_2^\dagger(-\mathbf{k}_j)|0\rangle.$$

If each pair of particles has (non-negative) probability $P(\mathbf{k}_j)$ of being emitted by the source, the resulting *incoherent statistical mixture* is described by the following density matrix:

$$\rho_{12} = \sum_{\mathbf{k}_j} P(\mathbf{k}_j) |\Psi_j\rangle_{12} \langle\Psi_j|_{12} = \sum_{\mathbf{k}_j} P(\mathbf{k}_j) \rho_1^j \otimes \rho_2^j \quad (6)$$

where $\rho_1^j = |\mathbf{k}_j\rangle_1 \langle\mathbf{k}_j|_1$ and $\rho_2^j = |-\mathbf{k}_j\rangle_2 \langle-\mathbf{k}_j|_2$ are the density matrices for particles 1 and 2, respectively, belonging to the j^{th} pair. It is well known that for each particle to propagate with such a perfectly well defined momentum, the sources have to be infinite in the transverse direction [15, 16]. Therefore, pairs of particles with a perfect momentum-momentum correlation do not exhibit any position-position correlation. Indeed, if ρ_{12} in Eq. (6) is expressed in the position base, it becomes, assuming $P(\mathbf{k}_j) = P$ constant: $\rho_{12} = P \rho_1^{(\mathbf{r}_1)} \otimes \rho_2^{(\mathbf{r}_2)}$, which is just the product of two *uncorrelated* density matrices, one for each particle. In the more realistic case of finite transverse dimension of the source, the position-position correlation improves at the expenses of the momentum-momentum correlation: each particle is always diffracted independently in such a way that no correlation between the uncertainties $\Delta(\mathbf{k}_1)$ and $\Delta(\mathbf{k}_2)$ can be achieved. Note that the position-position correlation improves in the sense that each particle can now be localized in a finite area, but its localization is still independent on the localization of the other particle from the same pair, i.e., no correlation between the uncertainties $\Delta(\mathbf{r}_1)$ and $\Delta(\mathbf{r}_2)$ can be achieved. In general, any attempt to improve the classical correlation in one variable inevitably worsens the correlation in the other. In conclusion, any source of classically correlated pairs of particles: i) can never achieve perfect correlation in both momentum and position variables; ii) can never satisfy inequality Eq. (2).

In summary, we have experimentally demonstrated that SPDC photon pairs satisfy the EPR-type non-classicality condition Eq. (2). In doing so, we have shown that entangled particles exhibit almost perfect momentum-momentum *and* position-position correla-

tions. Classically correlated pairs of particles cannot exhibit such behavior. The measurement described in this Letter thus provides a direct way to distinguish between quantum entanglement and classical correlation in momentum and/or position variables. An important practical consequence is that only the non-local correlation implicit in entangled systems allows to ‘overcome’ the usual diffraction limit and to obtain super-resolved images, as proposed and demonstrated in Ref. [8, 9, 16]. Furthermore, our experiment shows that a distinction between classically correlated and quantum entangled systems, in momentum and/or position variables, can be realized experimentally through the study of ‘ghost’ imaging-type experiments [17]. This is a quite different approach with respect to Bell’s inequality and may represent an extension of Bell’s inequality, in optics.

The authors thank M.H. Rubin and V. Protopopescu for helpful comments and discussions. This work was supported, in part, by ARDA, NASA-CASPR program, NSF, and ONR. The Oak Ridge National Laboratory is managed by UT-Battelle, LLC, for the U.S. DOE under contract DE-AC05-00OR22725.

-
- [1] E. Schrödinger in *Quantum Theory and Measurement*, J.A. Wheeler and W.H. Zurek, eds. (Princeton Univ. Press, New York, 1983).
 - [2] A. Einstein, B. Podolsky, and N. Rosen, Phys. Rev. **47**, 777 (1935).
 - [3] D.N. Klyshko, *Photon and Nonlinear Optics*, (Gordon and Breach Science, New York, 1988).
 - [4] J.P. Dowling and G.J. Milburn, quant-ph/0206091; A. Migdall, Phys. Today **52**, 41 (1999).
 - [5] D.V. Strekalov *et. al.*, Phys. Rev. Lett. **74**, 3600 (1995).
 - [6] T.B. Pittman *et. al.*, Phys. Rev. A **52**, R3429 (1995).
 - [7] V. Giovannetti, S. Lloyd, and L. Maccone, Phys. Rev. A **65**, 022309 (2002); Y. Shih (unpublished).
 - [8] A.N. Boto, P. Kok, D.S. Abrams, S.L. Braunstein, C.P. Williams, and J.P. Dowling, Phys. Rev. Lett. **85**, 2733 (2000).
 - [9] M. D’Angelo, M.V. Chekhova, and Y. Shih, Phys. Rev. Lett. **87**, 013602 (2001).
 - [10] R.S. Bennink, S.J. Bentley, and R.W. Boyd, Phys. Rev. Lett. **89**, 113601 (2002).
 - [11] Z.Y. Ou, S.F. Pereira, H.J. Kimble, and K.C. Peng, Phys. Rev. Lett. **68**, 3663 (1992). Further references can be found in this article.
 - [12] M.H. Rubin, D.N. Klyshko, Y.H. Shih, and A. V. Sergienko, Phys. Rev. A **50**, 5122 (1994).
 - [13] M.H. Rubin, Phys. Rev. A **54**, 5349 (1996).
 - [14] M.H. Rubin, quant-ph/0303188.
 - [15] D. Bedford and F. Selleri, Lett. Nuovo Cimento **42**, 325 (1985); M.J. Collet and R. Loudon, Nature **326**, 671 (1987).
 - [16] Y.-H. Kim and Y.H. Shih, Found. Phys. **29**, 1849 (1999).
 - [17] Cancellation of all first order effects is a prerequisite for making such a distinction since quantum ‘ghost’ interference-imaging phenomena are second order effects.